

Contribution of charge-density-wave phase excitations to thermal conductivity below the Peierls transition

A. Smontara and K. Biljaković

Institute of Physics of the University of Zagreb, P. O. Box 304, 41001 Zagreb, Croatia

S. N. Artemenko

Institute of Radioengineering and Electronics, Russian Academy of Sciences, Mokhovaya 11, 103907, Moscow, Russia

(Received 19 October 1992; revised manuscript received 29 March 1993)

We report on measurements of the thermal conductivity of the quasi-one-dimensional conductor $(\text{NbSe}_4)_{10}\text{I}_3$ between 80 and 320 K. We show that the thermal conductivity exhibits a well-defined minimum below the Peierls transition temperature $T_p = 285$ K. Such behavior has also been found in the charge-density-wave (CDW) conductors $\text{K}_{0.3}\text{MoO}_3$ and $(\text{TaSe}_4)_2\text{I}$, and seems to be a generic property of CDW systems. We propose that this feature results from the contribution of low-frequency phasons of rather large velocity. The position of the minimum in the thermal conductivity corresponds to the temperature range where the screening of the Coulomb interaction by the quasiparticles (electron-hole pairs) becomes effective and consequently enables the phason contribution.

I. INTRODUCTION

The collective oscillation spectrum in the charge-density-wave (CDW) conductors was first presented in the work of Lee, Rice, and Anderson.¹ They showed that the Peierls transition leads to a modification of the phonon spectrum at $\mathbf{Q} = 2k_F$, which is the CDW wave vector, and to the appearance of two new modes of oscillations. In the long-wavelength limit, one of them corresponds to the amplitude and the other to the phase oscillations of the order parameter with an acoustic dispersion $\omega_\phi = v_F |q - 2k_F|$. It was also shown that at $T = 0$ the disappearance of dielectric screening leads to a finite phason frequency; then, according to theoretical predictions, the phason spectrum should be modified due to the screening effects caused by quasiparticles.²⁻⁶ These effects must show up most clearly in the Peierls conductors, when exhibiting a semiconducting energy spectrum. The screening effects give rise to drastic (i.e., exponentially) temperature dependence of some kinetic characteristics, such as the nonlinear conductivity in CDW conductors,⁵ since the free-carrier concentration diminishes exponentially on cooling down to $T < T_p$. The elasticity associated with the phase deformations of the collective mode, recently measured by inelastic neutron scattering,⁷ unambiguously proves that Coulomb forces play an important role in the intrachain CDW deformation processes. There is no other experimental evidence on the change of the phason spectrum.

Due to their high velocity, which few times may exceed the steepest acoustic mode, phasons should contribute to thermal conductivity. Previous papers on thermal conductivity of different CDW systems pointed out the fact that anomalous behavior around T_p cannot be explained only in the frame of carrier and lattice contributions. Here, we elaborate on the possibility that the contribution from the thermally assisted phason motion is the

missing link for a better description of the thermal conductivity of these systems. Also, our results of thermal conductivity of some CDW compounds in the frame of the proposed interpretation might give an indirect experimental indication that the phason spectrum is strongly affected by quasiparticle screening processes.

II. THERMAL CONDUCTIVITY OF $(\text{NbSe}_4)_{10}\text{I}_3$

We have measured the thermal conductivity of the CDW compound $(\text{NbSe}_4)_{10}\text{I}_3$ between 80 and 320 K. This compound, as well as $(\text{TaSe}_4)_2\text{I}$ and $(\text{NbSe}_4)_3\text{I}$, consists of MX_4 parallel chains separated by iodine atoms. The incomplete d_z band filling of the Nb and Ta atoms is amenable to the Peierls distortion.⁸ Such a transition has been detected in $(\text{NbSe}_4)_{10}\text{I}_3$ at $T_p = 285$ K (Ref. 9) and at $T_p = 260$ K in $(\text{TaSe}_4)_2\text{I}$.⁸ Though structurally akin with both compounds, $(\text{NbSe}_4)_3\text{I}$ does not undergo such a transition but rather exhibits a ferrodistorptive structural phase transition at $T_c = 274$ K (Ref. 8) and remains a semiconductor in the whole temperature range with the largest gap within the MX_4 family. The thermal conductivity of this compound is included for comparison purposes.

The technique we used for thermal conductivity measurements is a standard four-contact method, relative to a constant foil.^{10,11} Typical dimensions of the sample were $2.5 \times 0.3 \times 0.5$ mm³. The sample holder was closely surrounded by the heat shield, whose temperature was controlled so as to differ less than 0.5 K from the sample temperature, which minimized the radiation heat losses. The cooling (heating) rate was ~ 5 K/h, and even less than 1 K/h in the transition region. The temperature difference along the sample was always smaller than 1 K (0.2 K in the transition region). The relative accuracy of the measurement was 1–2%, much better than the absolute one which was 20% (mainly due to the uncertainty

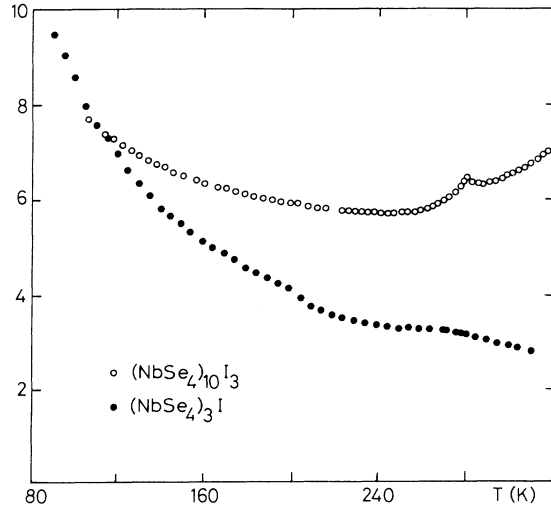


FIG. 1. Thermal conductivity λ as a function of temperature for $(\text{NbSe}_4)_{10}\text{I}_3$ (\circ) and $(\text{NbSe}_4)_3\text{I}$ (\bullet). The thermal conductivity of the CDW compound $(\text{NbSe}_4)_{10}\text{I}_3$ shows a well-defined minimum below the Peierls transition.

in defining the geometrical factor of thin samples).

The measured total thermal conductivity of $(\text{NbSe}_4)_{10}\text{I}_3$ and $(\text{NbSe}_4)_3\text{I}$ in the temperature range from 80 to 320 K is shown in Fig. 1. The thermal conductivity of $(\text{NbSe}_4)_3\text{I}$, which does not undergo a Peierls distortion, increases almost monotonically with decreasing temperature.¹⁰ In contrast, the thermal conductivity of $(\text{NbSe}_4)_{10}\text{I}_3$ shows a well-defined minimum in the region of the Peierls transition and a weak anomaly of few percent of the total conductivity at T_p .

III. COMPARISON WITH OTHER CDW COMPOUNDS

The recognized general behavior of the thermal conductivity of $(\text{NbSe}_4)_{10}\text{I}_3$, characterized by a broad minimum in the region of the Peierls transition and a weak anomaly just below T_p ,^{11,12} appears also in the thermal conductivity of TaS_3 ,^{13,14} $\text{K}_{0.3}\text{MoO}_3$,^{12,15-18} as well as in $(\text{TaSe}_4)_2\text{I}$ ^{11,12,17} indicating that the origin of this generic feature might be due to the presence of the CDW's.

Possible physical explanations for this effect have been already considered¹¹⁻¹⁸ and it has been pointed out that the anomaly at T_p cannot be accounted for by considering only the electronic and phononic contribution to the thermal conductivity, but no satisfactory explanation has been given yet. It is very well known that on lowering the temperature through the Peierls transition temperature the electronic spectrum is drastically changed and the CDW gap appears at the Fermi surface. An exponential decrease occurs in the thermodynamical quantities (including thermal conductivity) below the transition temperature brought about by the spectrum of the quasi-particle excitations of the condensed phase, i.e., the bound electron-hole pairs of the CDW state. Because all

the properties for screening are controlled by the gap amplitude E_g , we will make a detailed comparison between $(\text{NbSe}_4)_{10}\text{I}_3$ ($E_g = 3700$ K) and blue bronze ($E_g = 960$ K and $T_p = 180$ K). One expects for the former a very fast temperature change and for the latter a relatively wide range for the determination of all relevant contributions to the thermal conductivity. In addition, rather detailed investigations by inelastic neutron scattering of blue bronze provide some necessary data for testing our assumptions.

IV. CONTRIBUTIONS TO THE THERMAL CONDUCTIVITY OF CDW SYSTEMS

We turn now to discuss the various contributions to the thermal conductivity of CDW systems.

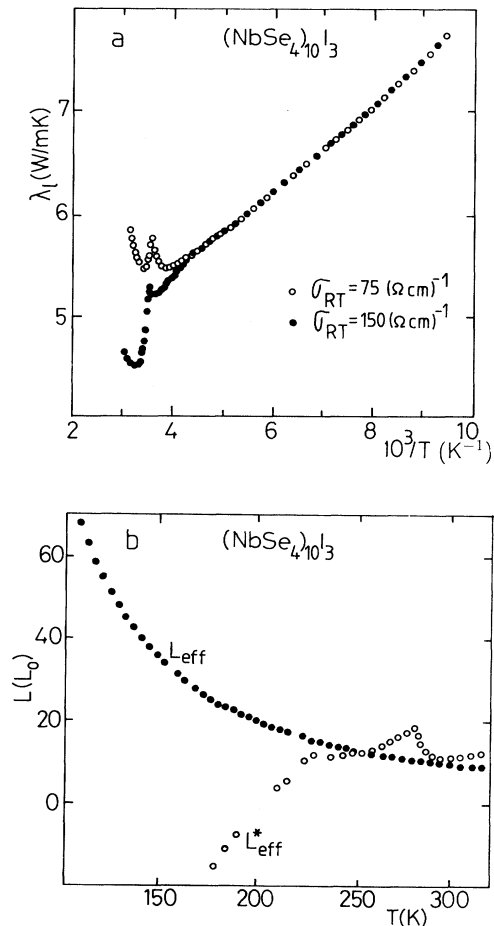


FIG. 2. (a) The lattice contribution $\lambda_l = \lambda - \lambda_{fc}$ vs $1000/T$ for two different σ_{RT} for $(\text{NbSe}_4)_{10}\text{I}_3$; $75 (\Omega \text{ cm})^{-1}$ (\circ) and $150 (\Omega \text{ cm})^{-1}$ (\bullet) cannot be fitted by simple T^{-1} law. There is almost no influence of λ_{fc} below 220 K. (b) The effective Lorentz numbers (Wiedemann-Franz ratios) for $(\text{NbSe}_4)_{10}\text{I}_3$. $L_{\text{eff}} = \lambda_{fc}/\sigma T$ (\bullet) defined by Eq. (1) and L_{eff}^* (\circ), as explained in the text, show different tendencies at lower temperatures.

A. Lattice contribution

The lattice contribution λ_l to thermal conductivity in this temperature range is due both to the umklapp processes and normal one.¹⁹ The last one does not by itself cause thermal resistance but nevertheless contributes to it indirectly by distributing momentum among all the phonons. It has to be pointed out here that we anticipate that there are no modifications of the “normal” phonons by the phonon modes becoming “soft” as well as that optical phonons do little to contribute to thermoconductivity. This is not totally obvious in the case of low-lying optical mode, such as the amplitude mode. Although we are aware of the possible shortcomings of this treatment in the case of the lattice conductivity of CDW systems, nevertheless, we follow the analysis of the lattice contribution used by other authors in this field.^{13–18}

The lattice conductivity $\lambda_l = \lambda - \lambda_{fc}$ can be determined with relatively high accuracy (better than 1%) regardless of the free-carrier contribution λ_{fc} , as illustrated in Fig. 2(a) for two extreme values of the room-temperature (RT) conductivity of $(\text{NbSe}_4)_{10}\text{I}_3$. The same figure shows that λ_l rather obeys the exponential law such as $\lambda_l = A \exp(\theta_D/\alpha T)$ (α is a numerical factor and θ_D is the Debye temperature), instead of following the T^{-1} law. So far, our findings are similar to the ones in Ref. 18. It seems that other authors^{13–17} did not pay special attention to the application of different fits. Debye temperatures of CDW systems are relatively low and they are inside the temperature range of our measurements [$\theta_D \approx 350$ K for $\text{K}_{0.3}\text{MoO}_3$, $\theta_D \approx 116$ K for $(\text{NbSe}_4)_3\text{I}$, $\theta_D \approx 124$ K for $(\text{TaSe}_4)_2\text{I}$, and $\theta_D \leq 200$ K as anticipated for $(\text{NbSe}_4)_{10}\text{I}_3$] but the condition $T < \theta_D$ (Ref. 20) is roughly fulfilled.

The parameters obtained from the fit for the lattice contribution for blue bronze are $A = 0.98$ W/mK and $\theta_D/\alpha = 174$ K. As α is the numerical factor of the order of 2,^{20,21} we get for $\alpha = 2$ and $\theta_D = 350$ K an excellent agreement with the obtained value. For $(\text{NbSe}_4)_{10}\text{I}_3$, $A = 4.24$ W/mK and $\theta_D/\alpha = 62.7$ K. If we take the same $\alpha = 2$ obtained for blue bronze, then the Debye temperature of $(\text{NbSe}_4)_{10}\text{I}_3$ deduced from our thermal conductivity measurement should be $\theta_D \approx 125$ K, quite close to the value of θ_D for $(\text{TaSe}_4)_2\text{I}$.

It is important to notice that we took the largest possible lattice contribution and that a T^{-1} fit would give smaller values. The solid lines in Figs. 3 and 4 are the extrapolation of our fits at higher temperatures. A well-defined excess to λ_l is present around and above T_p .

B. Free-carrier contribution

We pay special attention to the estimate of the free-carrier contribution, λ_{fc} , as for $T > T_p$ $(\text{NbSe}_4)_{10}\text{I}_3$ shows a semiconducting and blue bronze a metallic behavior of electrical conductivity. In the absence of a more quantitative, rigorous treatment of the electronic contribution, it may be helpful to use the often suggested analogy between the CDW systems and semiconductors with a temperature-dependent gap.²² In this case, besides the usual Wiedemann-Franz (WF) contribution (the polar

term), which has been considered as the only one by other authors,^{13–18} the bipolar part of the electron-hole pairs should be added²³ and modified as in the following because of the temperature-dependent effective gaps:²⁴

$$\lambda_{fc} = \frac{\pi^2}{3} \left[\frac{k_B}{e} \right]^2 \sigma T + \frac{b}{(b+1)^2} \left[\frac{E_g}{k_B T} + 4 \right] \times \left[-T \frac{d(E_g/k_B T)}{dT} + 4 \right] \left[\frac{k_B}{e} \right]^2 \sigma T, \quad (1)$$

where e is the electronic charge, σ the electrical conductivity, E_g the temperature-dependent effective Peierls gap,²² and b the electron-hole mobility ratio.

Even if it represents an improvement in the sense that the semiconducting behavior has been accounted for [especially for $(\text{NbSe}_4)_{10}\text{I}_3$ which has semiconducting properties above T_p but also for $\text{K}_{0.3}\text{MoO}_3$ as it shows the existence of the pseudogap above T_p], we should put some brackets on this assumption below T_p . In fact, the CDW branches of quasiparticle excitations are not particlelike and holelike (but rather bound states of particles and holes), and the main process of heat transport in semiconductors, the particle-hole recombination, is absent in CDW systems.

We have determined the parameters $\sigma(T)$, b , and $E_g(T)$ from separate measurements of electrical conductivity and thermopower (TEP) on the same crystals, which we used for thermal conductivity experiments. The obtained λ_{fc} contribution for both materials is plotted in Figs. 3(a) and 4(a). The self-consistent determination of both contributions, λ_l and λ_{fc} , in which the latter is probably (but on purpose) overestimated,²⁵ implies that there should exist an additional extra term. In other words, if one considers only two contributions, as $\lambda = \lambda_u + \lambda_{fc}$, the corresponding effective Lorentz number L_{eff}^* [$L_{\text{eff}}^* = (\lambda - \lambda_l)/\sigma T$] would exhibit an unphysical behavior when compared to the behavior given by Eq. (1), where $L_{\text{eff}}^*(L_0) = \lambda_l/\sigma T$ [$L_0 = 2.45 \times 10^{-8}$ W Ω K⁻² is the Sommerfeld value] as shown in Fig. 2(b). This figure is very illustrative for at least two reasons. It shows that L_{eff}^* , necessary for compensating all the residual conductivity at RT, needs to be more than $10L_0$ (a simple WF contribution is too small to be presented in Figs. 3 and 4). Even if one tentatively accepts the possibility of an inaccurate determination of electrical conductivity, what can only rescale the data, it is impossible to change the opposite tendency of L_{eff}^* to decrease at lower temperatures. This appears as a simple “mathematical artifact” manifesting the inconsistent analysis of the data when all possible contributions have not been taken into account and we have to conclude that both the free carriers and the “usual” phonon contributions cannot explain the upturn of λ 20 K below T_p and that an additional contribution is missing.

The insets in Figs. 3(a) and 4(a) show the extra thermal conductivities for $(\text{NbSe}_4)_{10}\text{I}_3$ and $\text{K}_{0.3}\text{MoO}_3$ when $\lambda_l + \lambda_{fc}$ has been withdrawn. These contributions have

almost the same magnitude as the free-carrier contributions.

As we pointed out above, it has been already found by other authors^{17,18} that the detailed temperature dependence of λ in blue bronze does not agree exactly with the sum of lattice and electronic contributions and it was only tentatively suggested that the peak in λ at T_p is a result of heat carried by soft phonons.

C. Phason contribution

We will now associate the conductivity in excess of the phonon and free-carrier contribution with excitations of the CDW systems, i.e., mainly phasons. Their spectrum is to a great extent determined by long-range Coulomb interaction since the deformation of the CDW phase produces an electric field which results in a displacement current and a quasiparticle current. The phason frequency is given by⁵

$$\omega^2 = \omega_0^2 \frac{\epsilon_{\parallel} k_{\parallel}^2}{(\epsilon_{\parallel} k_{\parallel}^2 + \epsilon_{\perp} k_{\perp}^2)} \frac{1}{\left[1 + \frac{\omega_r}{i\omega + Dk^2}\right]}, \quad (2)$$

where $\omega_0^2 = \frac{3}{2} \Lambda \omega_Q^2$. Here, ω_Q is the bare phonon frequency, ϵ_{\parallel} and ϵ_{\perp} are the dielectric constants parallel and perpendicular to the chain axis, $\omega_r = 4\pi\sigma/\epsilon_{\infty}$ is the frequency of the dielectric relaxation, and D is the diffusion constant.²⁶ Equation (2) is valid in a small- k limit. The finite value of ω_0 (where Λ is the dimensionless coupling strength of the electron-phonon interaction) and the factor containing ϵ_{\parallel} and ϵ_{\perp} in (2) originate from static dielectric screening. The denominator accounts for quasiparticle conductivity screening. This screening factor is effective at higher temperatures where the electric field produced by CDW deformation is screened by quasiparticle excitations, a condition fulfilled when the dielectric relaxation frequency ω_r exceeds the characteristic phason frequency⁵ $\omega_0 = \sqrt{3/2} \omega_A$ (ω_A is the amplitude mode frequency). This allows the low-frequency phasons to appear, which in the region $\omega_0/\sqrt{\omega_r D} < k < \sqrt{\omega_r/D}$ have a large velocity $s_{\parallel} = \omega_0 \sqrt{D/\omega_r}$ (Ref. 27) and a small damping. The contribution of phasons to thermal conductivity can be estimated from the usual Debye formula,

$$\lambda_{\text{ph}} \sim \int \tau \frac{s_{\parallel}^2 \omega^2 \exp\left[\frac{\hbar\omega}{k_B T}\right]}{T^2 \left[\exp\left[\frac{\hbar\omega}{k_B T}\right] - 1\right]^2} dk. \quad (3)$$

In order to estimate the transport relaxation time τ of phasons we use the inverse damping rate value Γ and take $\tau = (\Gamma + \omega_0^2/\omega_r)^{-1}$. Considering the parameters which have a weak temperature dependence in comparison with ω_r , we get for $\hbar\omega \ll k_B T$,

$$\lambda_{\text{ph}} \approx \sqrt{\omega_r D} \frac{1}{1 + \frac{\omega_r \Gamma}{\omega_0^2}}. \quad (4)$$

Γ reflects all the changes in the inverse phason lifetime, also including anharmonic processes²⁸ which are of non-Coulomb origin. When the ratio $\Gamma/(\omega_0^2/\omega_r)$ is small (the denominator is the damping originating from the Coulomb effects), the phason contribution to the thermal conductivity increases with T as $\lambda_{\text{ph}} \approx \sqrt{\omega_r D}$. If Γ exceeds Coulomb damping, one gets $\lambda_{\text{ph}} \approx (\omega_0^2/\Gamma) \sqrt{D/\omega_r}$, and the phason thermal conductivity decreases with increasing T .

Figures 3 and 4 demonstrate that there is a convincing coincidence between the position of the minimum in the thermal conductivity [Figs. 3(a) and 4(a)] and the temperature at which the required conditions for the effectiveness of phasons are fulfilled [$\omega_0 < \omega_r$ in Figs. 3(b) and 4(b)]. To calculate ω_r we used our results for the linear electrical conductivity σ , obtained on the same samples on which the thermal conductivity was measured and normalized according to the self-consistent analysis of thermal conductivity. For $(\text{NbSe}_4)_{10}\text{I}_3$ the measured

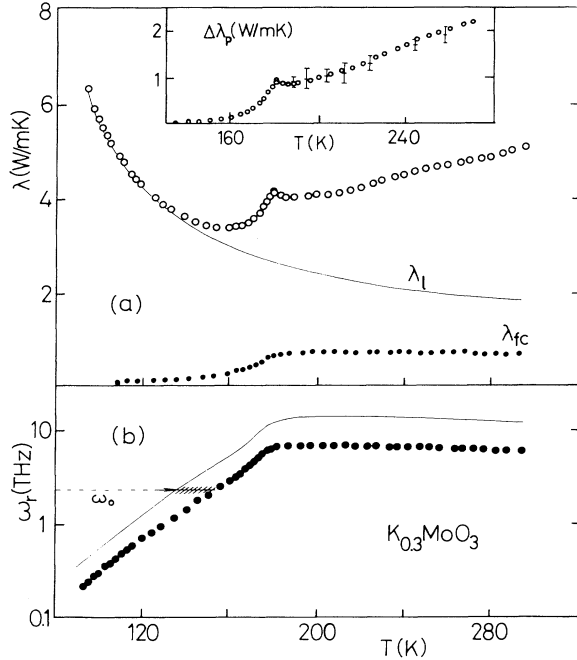


FIG. 3. (a) Thermal conductivity of $(\text{NbSe}_4)_{10}\text{I}_3$ (\circ) with all contributions estimated in a self-consistent analysis (see the text). λ_l represents the lattice contribution fitted to the formula $\lambda_l = A \exp(\theta/\alpha T)$ with $A = 4.24$ W/mK and $\theta/\alpha = 62.7$ K (—). λ_{fc} is the free-carrier contribution estimated from Eq. (1) (\bullet) with $\sigma_{\text{RT}} = 100$ ($\Omega \text{ cm}$)⁻¹ where for the ratio of mobilities we estimated $b = 0.32$ at $T < T_p$ from TEP measurements (Ref. 36) and for $Eg(T)$ we used the general form given in Ref. 22. The simple Wiedemann-Franz law gives almost 10 times smaller λ_{fc} at RT. $\Delta\lambda_p$ is the extra conductivity attributed to phase excitations (shown in the inset). (b) The frequency of dielectric screening ω_r vs temperature. The arrow indicates $\omega_0 = \omega_r$; $\omega_0 = 3.7$ THz (Ref. 33) being the phason frequency in the unscreened regime at $T = 0$. The shaded area shows the uncertainty of the parameters used for the analysis (—, $\epsilon_{\infty} = 15$; \bullet , $\epsilon_{\infty} = 30$).

$\sigma_{RT} = 100 (\Omega \text{ cm})^{-1}$ was in a good agreement with other authors.⁹ However, for blue bronze the value $\sigma_{RT} = 300 (\Omega \text{ cm})^{-1}$, measured on the same sample which was used for the thermal conductivity measurements, was relatively low but still inside a range of values measured by different authors in different samples. On another sample of blue bronze, cut from the same crystal as the sample for thermal conductivity, we have measured conductivity that was two times higher. This was the main reason to also probe the twice higher value²⁹ $\sigma_{RT} = 600 (\Omega \text{ cm})^{-1}$ [full line in Fig. 4(b)] and to see the probable region of uncertainty in defining ω_r [the shaded area in Fig. 4(b)]. Since significant uncertainties also exist for blue bronze in the value of ϵ_∞ (by different authors and for different samples), we took the average value from accessible sources ($\epsilon_\infty = 100$). The $\omega_0 = 2.2$ THz value has been obtained from neutron-scattering experiments.³⁰ Infrared measurements on the same sample on which we measured thermal conductivity gave for $(\text{NbSe}_4)_{10}\text{I}_3$ $\epsilon_\infty \approx 30$ which

is relatively large³¹ if compared with blue bronze according to the relation $\epsilon_\infty \sim (\omega_p/E_g)^2$, where ω_p is the plasma frequency determined by optical measurements.^{31,32} So, we took the twice smaller value $\epsilon_\infty = 15$ [full line in Fig. 3(b)] to demonstrate the possible region of ω_r values for $(\text{NbSe}_4)_{10}\text{I}_3$. The $\omega_0 = 3.7$ THz value for $(\text{NbSe}_4)_{10}\text{I}_3$ has been obtained from Raman experiment.³³

The region of the thermal conductivity minimum covers the temperature range in which the condition $\omega_0 = \omega_r$ is reached [indicated in Figs. 3(b) and 4(b) by the shaded area which also represents the uncertainties of the used parameters]. In $(\text{NbSe}_4)_{10}\text{I}_3$ this occurs at $260 \text{ K} < T < 270 \text{ K}$. For $\text{K}_{0.3}\text{MoO}_3$ this region is relatively larger ($140 \text{ K} < T < 160 \text{ K}$). The same analysis that we did for other CDW systems, such as $(\text{TaSe}_4)_2\text{I}$ and TaS_3 , gives additional confirmation for this assertion.³⁴

The maximum phason contribution appears at $\omega_r = \omega_0^2/\Gamma$. As in the classical description of an incommensurate Peierls instability, the amplitude and phase modes are characterized by the same damping²⁸ we can take for $\text{K}_{0.3}\text{MoO}_3$ $\Gamma \approx 0.8$ THz from neutron-scattering measurements.³⁰ Following ω_r from Fig. 4(b), the expected maximum in the phason contribution should occur at $T \approx 175 \text{ K}$. Furthermore, the phason thermal conductivity decreases very slowly with increasing temperature, as has been explained above. In the fluctuation region around T_p , contributions from other scattering processes may take place, and the application of the phason fit is not certain anymore. Unfortunately, there are no neutron-scattering data for $(\text{NbSe}_4)_{10}\text{I}_3$.

D. Thermal fluctuations above the Peierls transition

The heat current associated with CDW fluctuations gives rise in the chain direction to an excess thermal conductivity where the entropy is carried by the fluctuations themselves in what is manifested as the square-root cusp in the thermal conductivity at the CDW transition.³⁵ A similar cusp appears also in the free-carrier contribution as a consequence of the singularity of the derivative of the effective gap [Eq. (1)].³⁴ On the other hand, quasiparticle scattering due to fluctuations does not give rise to any singular term in the vicinity of the phase transition but it can give an almost linear increase at higher temperature,³⁵ which outlines the continuity of excitations through the second-order Peierls transition. At $T > T_p$, phonon damping comes dominantly from lattice anharmonicity²⁸ and the electron-phonon scattering which diminishes with increasing T . Thus, the origin of the increase of the lattice thermal conductivity above the Peierls transition results from the soft Kohn-Peierls phonons.

More information on the Kohn anomaly of blue bronze has been given in a very detailed neutron-scattering investigation.³⁰ When T decreases from room temperature toward T_p the damping Γ increases by a factor of 3. Γ demonstrates all scattering processes affecting the Kohn anomaly but it is mainly due to anharmonicity,²⁸ as mentioned above. If for the phonon relaxation time above T_p we take the inverse value of the measured damping

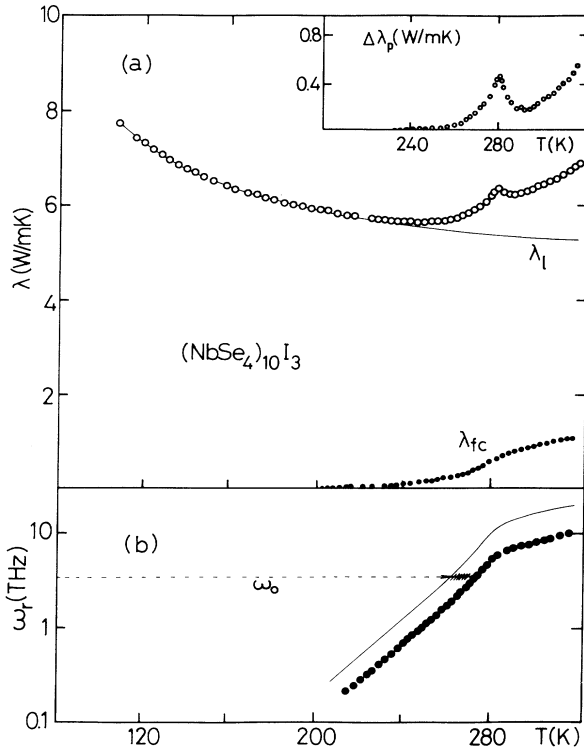


FIG. 4. (a) Thermal conductivity as a function of temperature for $\text{K}_{0.3}\text{MoO}_3$ (\circ) analyzed in the same manner as $(\text{NbSe}_4)_{10}\text{I}_3$. $\lambda_l = A \exp(\theta/\alpha T)$ is the lattice contribution with $A = 0.98 \text{ W/mK}$ and $\theta/\alpha = 174 \text{ K}$ (—). λ_{fc} is the free-carrier contribution (\bullet) with $b = 0.52$ and $E_g(T)$ from Ref. 22. $\Delta\lambda_p$ is the extra contribution due to phasons given in the inset. The crosses at $T > T_p$ represent normalized soft phonon contribution when the relaxation time is $\tau = \Gamma^{-1}$ [the damping, Γ , has been taken from neutron measurements (Ref. 30)]. (b) The frequency of dielectric screening ω_r vs temperature. The arrow indicates $\omega_r = \omega_0$ ($\omega_0 = 2.2$ THz, Ref. 30). $\sigma(T)$ has been used with two different values of σ_{RT} [—, $\sigma_{RT} = 600 (\Omega \text{ cm})^{-1}$; \bullet , $\sigma_{RT} = 300 (\Omega \text{ cm})^{-1}$].

rate,³⁰ then we can assume that the excess thermal conductivity above T_p varies as Γ^{-1} . The obtained temperature variation of $\Delta\lambda_p$ as shown in the inset of Fig. 4(a), is in very good relative agreement with the Γ^{-1} results from neutron scattering (shown by crosses in the same inset).

V. CONCLUSIONS

The CDW anomalies in thermal conductivity characterized by a small cusp at the Peierls transition temperature T_p and a deep minimum below T_p , reported in this paper for $(\text{NbSe}_4)_{10}\text{I}_3$ and $\text{K}_{0.3}\text{MoO}_3$ as representatives, present a generic feature of CDW systems. We give a detailed and self-consistent analysis of the lattice and free-carrier contribution and show that there is an additional contribution. The quasiparticle-phason interaction mechanism, which leads to phason screening, could provide a possible explanation for these anomalies. This raises a complex of intriguing questions which should in-

spire a more sophisticated theory of heat conduction in CDW systems.

Note added. Since the submission of this paper, K. Maki has published a calculation on excess thermal conductivity at the charge and spin-density-wave transition (considering only the amplitude mode)³⁵ where he also indicates that in the case of some generalization in his approach, new terms in the thermal conductivity associated with heat transport due to phasons can appear.

ACKNOWLEDGMENTS

The authors are grateful to P. Monceau, E. Tutiš, S. Barišić, and M. Apostol for many fruitful discussions and suggestions. They are thankful to J. R. Cooper for his support during the initial part of this work, and to B. Leontić and B. Gumhalter for a careful reading of the manuscript. This work was financially supported by the Ministry of Science of the Republic of Croatia (1.03.055) and EC contract CII-0526-M (CD).

¹P. A. Lee, T. M. Rice, and P. W. Anderson, *Solid State Commun.* **14**, 703 (1974).

²Y. Kurihara, *J. Phys. Soc. Jpn.* **49**, 852 (1980).

³S. N. Artemenko and A. F. Volkov, *Zh. Eksp. Teor. Fiz.* **80**, 2018 (1981) [*Sov. Phys. JETP* **53**, 1050 (1981)].

⁴K. Y. M. Wong and S. Takada, *Phys. Rev. B* **36**, 5476 (1987).

⁵S. N. Artemenko and A. F. Volkov, in *Charge Density Waves in Solids*, edited by L. P. Gor'kov and G. Grüner (Elsevier, Amsterdam, 1989), p. 365.

⁶A. Virosztek and K. Maki, *Synth. Met.* **57**, 4678 (1993).

⁷H. Hennion, J. P. Pouget, and M. Sato, *Phys. Rev. Lett.* **68**, 2374 (1992).

⁸P. Gressier, A. Meerschaut, L. Guemas, J. Rouxel, and P. Monceau, *J. Solid State Chem.* **51**, 141 (1984).

⁹Z. Wang, P. Monceau, M. Renard, P. Gressier, L. Guemas, and A. Meerschaut, *Solid State Commun.* **47**, 439 (1983).

¹⁰A. Smontara, K. Biljaković, L. Forro, and F. Lévy, *Physica* **143B**, 264 (1986).

¹¹A. Smontara, K. Biljaković, T. Futivić and T. Idžotić, *Fizika* **21**, Suppl. 1, 84 (1987); A. Smontara, K. Biljaković and F. Lévy, *ibid.* **21**, Suppl. 3, 127 (1989); A. Smontara, *Ž. Bihar*, and K. Biljaković, *Synth. Met.* **41**, 3981 (1991).

¹²A. Smontara, Ph.D. Thesis, University of Zagreb, 1991.

¹³A. V. Inyushkin, A. N. Taldenkov, and V. V. Florentiev, *Synth. Met.* **19**, 843 (1987).

¹⁴R. S. Kwok and S. E. Brown, *Fizika* **21**, Suppl. 3, 131 (1989).

¹⁵E. B. Lopes, M. Almeida, J. Dumas, and J. Marcus, *Phys. Lett. A* **130**, 98 (1988); E. B. Lopes, M. Almeida, J. Dumas, and J. Marcus, *Synth. Met.* **29**, F219 (1989).

¹⁶E. B. Lopes, M. Almeida, and J. Dumas, *Phys. Rev. B* **42**, 5324 (1990).

¹⁷R. S. Kwok and S. E. Brown, *Phys. Rev. Lett.* **63**, 895 (1989).

¹⁸S. M. De Land and G. Mozurkewich, *Solid State Commun.* **72**, 245 (1989).

¹⁹J. Ranninger (private communication).

²⁰R. E. Peierls, *Ann. Phys. (N.Y.)* **3**, 1055 (1929).

²¹P. G. Klemens, *Solid State Phys.* **7**, 1 (1958).

²²D. C. Johnson, *Phys. Rev. Lett.* **52**, 2049 (1984); *Solid State Commun.* **56**, 439 (1985); D. C. Johnson, J. P. Stokes, and R. A. Klemm, *J. Magn. Magn. Mater.* **54-56**, 1317 (1986).

²³P. J. Price, *Philos. Mag.* **46**, 1252 (1955).

²⁴R. A. Smith, *Semiconductors* (Cambridge University Press, Cambridge, 1978), p. 175.

²⁵For the sake of simplicity, we ignored the fact that the polar part which also applies, as it stands in Eq. (1), to a degenerate semiconductor, might change. Below T_p one has a nondegenerate semiconductor and the proportionality constant $\pi^2/3$ should be replaced by 2 (Ref. 24). Similarly, together with the bipolar part, we probably overestimated the free-carrier contribution which makes our final conclusion on the existence of an additional contribution qualitatively stronger.

²⁶The diffusion constant D is, in fact, temperature dependent and $D = (v_F^2/\gamma_0)(2/\pi)^{1/2}(T/\Delta)^{3/2}$ for $\Delta \gg T$.

²⁷This theoretical expression with $\gamma_0 = 3 \times 10^8 \text{ } \Omega/\text{s}^2$ fits nicely with the experimental results given in Ref. 7.

²⁸E. Tutiš and S. Barišić, *Phys. Rev. B* **43**, 8431 (1991).

²⁹However, a two times higher σ_{RT} value would also change slightly other contributions but more λ_l than $\Delta\lambda_p$ which remains qualitatively the same.

³⁰J. P. Pouget, B. Hennion, C. Escribe-Filippini, and M. Sato, *Phys. Rev. B* **43**, 8421 (1991).

³¹H. P. Geserich (private communication) [for $(\text{NbSe}_4)_{10}\text{I}_3$: $30 < \epsilon_\infty < 50$].

³²G. Travaglini and P. Watcher, *Phys. Rev. B* **30**, 1971 (1984).

³³T. Sekine, M. Izumi, and E. Matsura, *Synth. Met.* **19**, 869 (1987).

³⁴K. Biljaković *et al.* (unpublished).

³⁵K. Maki (private communication); *Phys. Rev. B* **46**, 7219 (1992).

³⁶A. Smontara, K. Biljaković, J. Mazuer, P. Monceau, and F. Lévy, *J. Phys. Condens. Matter* **4**, 3273 (1992).